



ELSEVIER

J. Non-Newtonian Fluid Mech. 85 (1999) 229–247

**Journal of  
Non-Newtonian  
Fluid  
Mechanics**

## Capillary rheometry of micellar aqueous solutions

Sergio Hernández-Acosta<sup>a</sup>, Alejandro González-Alvarez<sup>a</sup>, Octavio Manero<sup>b</sup>,  
Arturo F. Méndez Sánchez<sup>c</sup>, José Pérez-González<sup>c</sup>, Lourdes de Vargas<sup>c,\*</sup>

<sup>a</sup>*Departamento de Ingeniería Química, Universidad de Guadalajara, Guadalajara, Mexico*

<sup>b</sup>*Instituto de Investigaciones en Materiales, Universidad Nacional Autónoma de México, México*

<sup>c</sup>*Departamento de Física, Escuela Superior de Física y Matemáticas, Instituto Politécnico Nacional,  
C.P. 07300, Apdo. Postal 75-685, México D.F., México*

Received 6 July 1998; received in revised form 20 October 1998

---

### Abstract

In this work, the capillary flow of wormlike micellar solutions was studied in detail. Flow curves obtained with capillaries of different sizes for surfactant aqueous solutions at various concentrations, were analyzed with particular attention to the regions of flow instability. It was found that to observe unstable flow a critical residence time of the solution in the capillary is needed, in addition to a critical shear stress value. At specific surfactant concentrations, a plateau-like region was observed for sufficiently long residence times of the liquid under flow, either in the capillary or in a cone and plate rheometer. For shear rates higher than those of the plateau region, the expected upturn on the flow curves was observed and studied. The flow curves in this regime were dependent on the capillary diameter in an opposite way as found in the presence of slip, i.e., adherence appears to occur. The flow instabilities (observed as unstable pressure at the capillary entrance and a variable flow rate at the exit) were detected even for the lowest concentration solution where the plateau region was not apparent. The flow instabilities took place completely in the absence of slip. A remarkable effect was observed in the solution with the higher surfactant concentration using a flow system that allows long residence times (about 1 h). In this case, within a small window of shear stresses, a dramatic increase in flow rate accompanied by a large drop in the pressure measured at the capillary entrance was observed. After a minimum, the pressure increased again up to the initial stress and a new cycle began subsequently. This result is consistent with similar observations made in cone and plate or Couette geometries, which are attributed to the presence of 'shear bands'. © 1999 Elsevier Science B.V. All rights reserved.

---

### 1. Introduction

Wormlike micellar systems show a complex non-linear viscoelastic behaviour under shear flow. Phenomena flow instabilities, such as spurt flow and fluid structuration are often observed in micellar systems. Several authors [1–3] have pointed out that for shear rates or shear stresses larger than a

---

\* Corresponding author. E-mail: lvega@esfim.ipn.mx

critical value, a nearly constant stress plateau where the flow becomes unstable is observed. The existence of the plateau in the flow curve has been associated with a constitutive instability, i.e., a non-monotonic constitutive equation. It has been suggested that to maintain a steady flow along this region, the system may split into shear bands of low and high shear rates, and that the high shear rate band is a shear-induced (metastable) nematic phase [4]. From birefringence experiments under shear [5,6], the existence of the plateau has been interpreted as the coexistence of two stable phases within the solution under flow, one being isotropic and the other nematic. Meanwhile, the flow curve has been divided into three regions belonging to low, intermediate and high shear rates, wherein the material behaves as isotropic, two-phases and nematic, respectively.

The shear bands in the plateau region have been observed by optical methods [5–9] and nuclear magnetic resonance imaging (NMRI) [10]. In the high shear rate region past the plateau, an important element in the behaviour of wormlike surfactants concerns the nature of the upturn in the stress. The study of this region in rotational rheometers, by means of which most of the studies on the flow of wormlike micellar systems have been carried out, is limited by flow instabilities. To our knowledge, just a few experiments have been performed on the flow of wormlike micelles in confined geometries (capillaries and Couette cells). These experiences in part were aimed to study drag reduction [11] and to find evidences of spurt flow or apparent slip by NMRI [12]. The velocity distributions in capillary flow using this technique allowed for the analysis of discontinuities in the velocity profile. A ‘jump’ in the velocity near the walls was attributed to a band of high shear rate which arises from a discontinuity in the pressure drop-flow rate relationship once a critical stress or shear rate is exceeded. The origin of the shear band appearing close to the wall was associated with the bulk constitutive properties of the liquid and not to the boundary slip layer [12]. However, data available are insufficient to establish the process by which a banded flow develops from an initially homogeneous fluid. On the other hand, the presence of apparent slip in the Couette and capillary geometries in [12] was inferred from the analysis of velocity profiles. However, it must be born in mind, that a constitutive instability and slip often predicts similar effects, like a sudden increase in the flow rate. Finally, attention was not paid in [12] to the residence time of the liquid in the capillary, nor to entrance effects associated with the contraction flow prior to the capillary region.

It is the aim of the present investigation to systematically analyze the capillary flow of cetyltrimethylammonium tosilate (CTAT) solutions, made at various surfactant concentrations, by using capillaries of different diameters and length to diameter ratios. The observation of flow instabilities to identify the banded flow and their relationship with the critical stress and residence time of the liquid in the capillaries are the most important objectives of this work. The hypothesis of a critical residence time is particularly supported by means of cone and plate experiments. In addition, the relation between slip and flow instabilities is investigated for these solutions with the purpose of distinguishing slip from constitutive instabilities. Finally, visualization of the flow close to the capillary entrance and of spurt instabilities is performed.

## **2. Experimental**

The capillary rheometer consists of a transparent cubic reservoir of 1000 ml capacity to which glass capillaries can be attached [13]. Capillaries of 0.05, 0.12 and 0.30 cm in diameter and  $L/D = 400$  were utilized to look for slip, as well as capillaries of  $L/D = 50, 100$  and 400 to study the influence of

residence time and end effects on the flow. Reservoir to capillary contraction ratios ranged from 33 to 202. The experiments were performed at constant pressure drop, which was measured between the capillary ends by means of a differential pressure transducer within the range of 6880 Pa. Variations in the pressure transducer calibration were within at most 1%. The volumetric flow rate was determined by catch and measure. In ordinary conditions, the flow rate was determined within 1%. The experiments were carried out at  $T = 30^\circ\text{C}$ , that is above the Kraft temperature for the studied system.

Cetyltrimethylammonium tosilate (CTAT) from Sigma, with a purity of 98% was used as received. Samples were prepared by dissolving appropriate amounts of the surfactant in triple distilled water to obtain concentrations of 1.0, 1.5 and 2.0 w%, and thereafter the solutions were stored in glass bottles and placed in a water bath at  $50^\circ\text{C}$  for one week. They were shaken frequently to speed up homogenization and placed in a water bath for 3 days at the measurement temperature before experimentation.

To allow for very large variations in the residence time of the liquid in the flow system, two arrangements were considered. In the first one, the pressure-driving box was coupled to a cubic reservoir, to which the capillary was attached, by a 10 cm hose. In the second one, the pressure-driving box was connected to the cubic reservoir by another hose, 137 cm long, with a  $L/D$  ratio of 274. This system allows for a residence time of the order of hours.

In addition to capillary experiments, measurements were carried out in a cone and plate rheometer (Brookfield, DVIII) using cones of  $3^\circ$  with 1.2 and 2.4 cm radius and  $1.565^\circ$  with 1.2 cm radius.

Finally, video images were obtained of the spurt instabilities of the flow field close to the contraction in the capillary rheometer. Selected images were digitalized and printed.

### 3. Results and discussion

The apparent wall shear rate  $(\dot{\gamma})_{\text{app}}$  and the wall shear stress  $(\tau_w)$  were obtained by using the standard formulae:

$$\dot{\gamma}_{\text{app}} = \frac{32Q}{\pi D^3}, \quad (1)$$

$$\tau_w = \frac{\Delta p}{4(L/D)}, \quad (2)$$

where  $Q$  is the volumetric flow rate,  $D$  the capillary diameter,  $L$  the capillary length and  $\Delta p$  is the pressure drop between capillary ends. No corrections were applied to the flow data.

#### 3.1. Diameter dependence

##### 3.1.1. 1% solution

The flow curves for the three aqueous solutions are shown in Figs. 1–3. The behaviour displayed by these curves is very rich and interesting. Fig. 1 shows results for the 1% CTAT solution obtained with capillaries of diameters  $D = 0.05, 0.12$  and  $0.30$  cm and  $L/D = 400$ . The flow curves are free of end effects due to the large  $L/D$  ratio. They show four regions of flow behaviour, bounded by arrows lines,

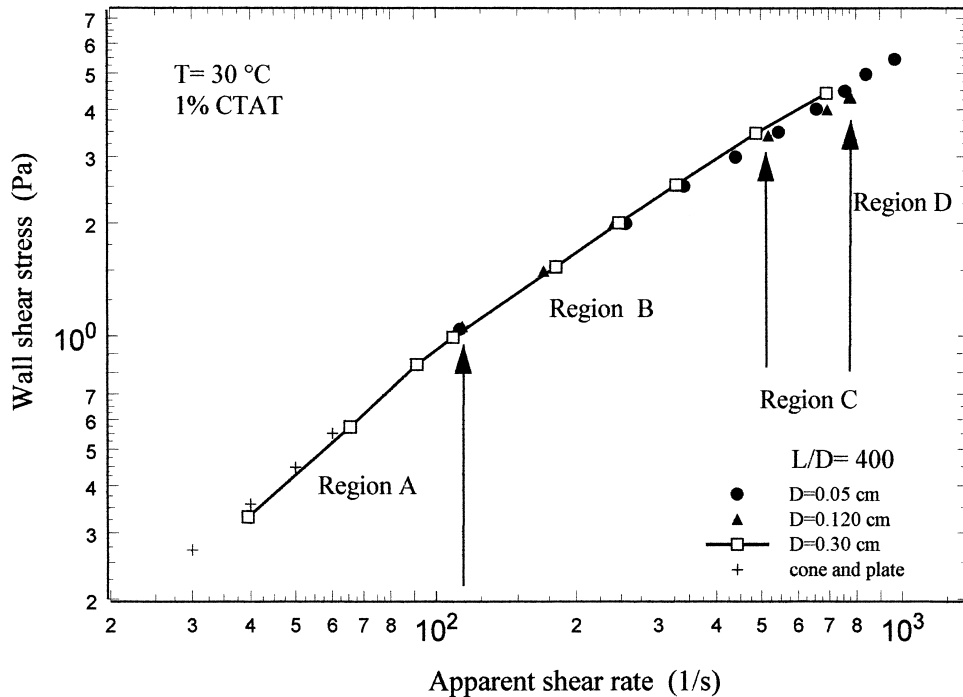


Fig. 1. Apparent flow curves for 1% CTAT solution and  $L/D = 400$  at  $30^\circ\text{C}$ , together with cone and plate data. (A) Newtonian flow region; (B) transition power-law type region; (C) banded flow region; (D) unstable power-law type region.

which were labelled as A, B, C and D. Callaghan et al. [12] observed only three flow regions for their system, the observation of one additional region in the present work is perhaps due to the low surfactant concentration used.

In region A, a Newtonian behaviour is observed from the lowest shear rates up to  $100\text{ s}^{-1}$ . In region B the flow behaviour was stable and characterized by a power-law index of 0.8. This region corresponds to shear rates below  $440\text{ s}^{-1}$ , or otherwise shear stresses below 3 Pa. There is a superposition of the flow curves associated with the different capillary diameters in regions A and B. At still higher shear rates, in region C and D, the flow became unstable. Differences between these two regions are mainly that in region C both, the pressure and the shear rate, change continuously, while in region D only the shear rate oscillates. It should be noted here that the driving pressure was kept constant for a given shear rate. However, the measured pressure drop did not reach a stationary value. Instead, oscillations in pressure and flow rate were observed, which evidences the existence of flow instabilities. Oscillations in pressure drop and flow rate became dramatic at higher concentrations as it will be shown below. Evidence of slip was not observed for these data.

Superposition of flow curves in regions A and B and their separation in regions C and D clearly show that the initially homogeneous fluid is modified by the flow field at high stresses. This result is consistent with a possible fluid structuration. Note that clear evidence of slip was not observed even though the flow became unstable.

In the same Fig. 1, steady state data obtained with the cone and plate rheometer are shown. Note that these match the flow curve in the Newtonian range. This is a confirmation that both rheometers are

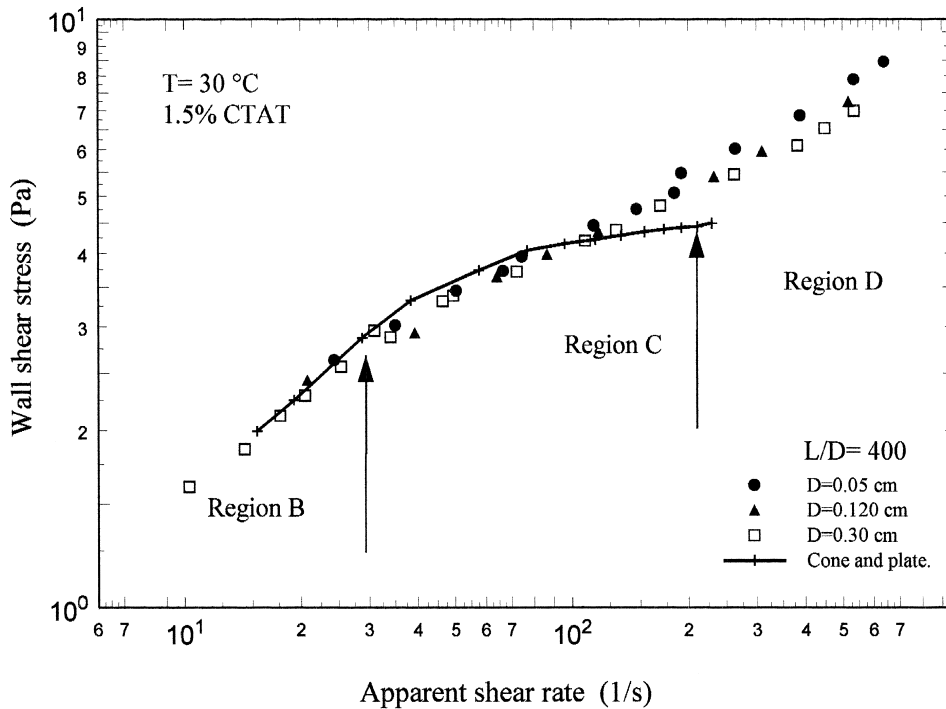


Fig. 2. Apparent flow curves for 1.5% CTAT solution and  $L/D = 400$  at  $30^\circ\text{C}$ , together with cone and plate data. (B) transition power-law type region; (C) banded flow region; (D) unstable power-law type region.

working properly. Shear rates higher than  $60\text{ s}^{-1}$  could not be attained with the cone and plate geometry since edge fracture occurred.

### 3.1.2. 1.5% solution

Fig. 2 shows results for the 1.5% CTAT solution where the same label pattern as in Fig. 1 was kept. In Fig. 2, the Newtonian region is not observed within the shear rates studied. A power-law type behaviour with a parameter  $n$  of 0.53 is observed in region B, which is bounded by a shear stress of about 3 Pa. At this stress value the slope of the flow curve decreases and signals a transition into the unstable region C. In region C, both shear rate and shear stress fluctuate in such a way that the data shown in the flow curve are not steady. However, they are representative of the flow behaviour in this region. At even higher shear rates, in region D, the shear rate oscillates within  $\pm 6\%$ , when the typical variations in steady flow are less than 1%; while the pressure drop varied by at most 2%. In this case it is impossible to consider that the pressure fluctuation is within experimental error, since in a steady flow measurement the pressure usually remains fixed.

In addition, in region D, the flow curves became diameter dependent, and show a clear tendency for the capillaries with smaller diameter to lie above those of larger diameter, i.e., there appear to be adherence or negative slip [14]. This result is the opposite to the usual behaviour in the presence of slip, and is in contrast with that happening in regions B and C, where the diameter does not have any effect on the flow curves.

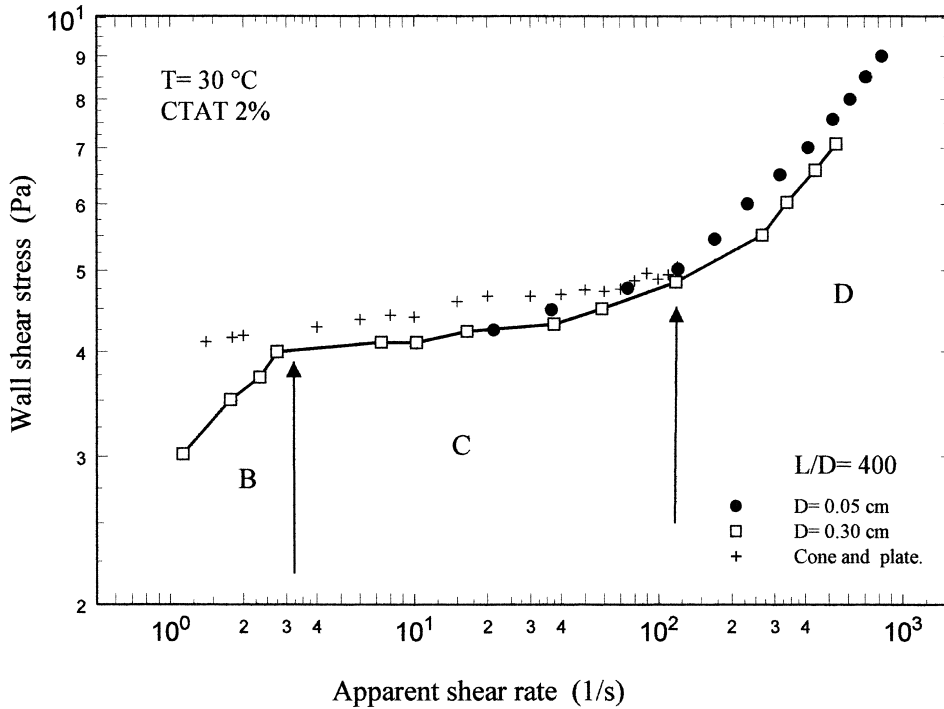


Fig. 3. Apparent flow curves for 2.0% CTAT solution and  $L/D = 400$  at 30°C, together with cone and plate data. (B) transition power-law type region; (C) banded flow region; (D) unstable power-law type region.

In Fig. 2 are also shown data corresponding to the cone and plate rheometer. It can be observed that cone and plate data cover only B and C flow regions, and the capillary data match those of the cone and plate in region B. This coincidence should not be found since capillary data are not Rabinowitsch corrected; in fact, capillary data should lie above those of cone and plate. This result may be interpreted as the beginning of fluid structuration, which may lead to a decrease in fluid viscosity. On the other hand, such structuration turns the fluid in a non-homogeneous one and therefore, an important conditions to have a true rheometric flow is violated. Thus region B appears to indicate a transition, where the second phase starts its nucleation due to flow.

The fluid structuration can also be inferred from the cone and plate data at the end of region C, wherein a plateau like region in the shear stress is reached. It is interesting to note that the plateau was not reached in the capillary experiment. This is due to the fact, as it will be shown later, that the fluid residence time in the capillary is not long enough to produce a high degree of structuration.

### 3.1.3. 2% CTAT solution

Fig. 3 shows data corresponding to the most concentrated solution (2%) where only three flow regions are observed. In this case the plateau region extends over a much wider span of shear rates. Here, it is possible to determine the critical stress for the onset of the plateau region and also the shear rates bounding the plateau. For shear stresses lower than the critical value (around 4 Pa) the behaviour is non-Newtonian (region B) and represents the transition region. The region C now shows a pronounced plateau in which banded flow has been reported [3]. In this region, again, instabilities and

spurt flow are detected and both, shear rate and shear stress fluctuate, being impossible to obtain a true steady state, as it happened in the case of the 1.5% CTAT solution. Data shown are only representative of the flow situation but not quantitatively reliable. For shear rates higher than those of the plateau, (region D) there is a second non-Newtonian unstable region where the magnitude of the stress at a given shear rate depends on the capillary diameter in the same fashion as in the 1.5% solution. In this region, the shear rate oscillates within at most  $\pm 10\%$  and the pressure drop within at most 1.5%.

The steady-state cone and plate data for this solution describe a wide plateau that covers over two decades in shear rate and lie above the capillaries data in regions B and C. In region B, the differences observed from both rheometers are due to the fact that cone and plate experiments were carried out at controlled shear rate, while capillary ones were performed at controlled pressure. In region C, the fluid residence time is larger in the capillary rheometer than the time interval between consecutive points in the cone and plate data. However, cone and plate data approach those of the capillaries at high shear rates when the residence time in capillaries becomes shorter and the upturn in the flow curves is observed. The upturn in the cone and plate rheometer flow curve is not observed because the fluid usually leaves the gap in this range of shear rates. In fact, it is possible that under no circumstances the upturn be observed in this geometry, since once the fluid separates into two phases, an equilibrium is reached because the fluid is not renewed as it occurs in the capillary. Callaghan et al. [10] reported observation of the onset of the upturn in a cone and plate rheometer. Experiments performed in our laboratory with a similar solution to that of Callaghan et al., in a Paar Physica cone and plate rheometer, showed that such observation of the upturn is coincident with the leaving of the solution from the gap, at shear rates where elastic effects began to be important and the highly elastic solution climbs on the cone.

This limitation of the cone and plate rheometer is overcome by using the capillary rheometer, in which the solution behaviour at high shear rates can be easily studied. The experimental evidence of the upturn in the shear stress and the trend of the flow curves for different capillary diameters at high shear rates had not been previously reported. Finally, observe again in Fig. 3 that the flow curve belonging to the capillary of smaller diameter lies above that of larger diameter, which shows the same trend as in the 1.5% solution. This result provides evidence of no slip behaviour.

The velocity profile in this region has been determined from the NMRI technique for CPyCl/NaSal by Mair and Callaghan [12] showing a plug type flow in the centre of the tube surrounded by another type of fluid layer of finite thickness. It was suggested that at high shear rates the formation of shear-induced structures is substantial on the capillary walls. This effect has been observed in the cone and plate geometry for sufficiently high shear rates [10]. Therefore, it is expected that the effective diameter of the capillaries will decrease due to adherence of this gel-like phase to the walls. Sometimes, a complete blocking of the capillary by the gel was observed in the present work, and this effect was more pronounced in the smallest capillary. Therefore, the pressure buildup will increase as the capillary diameter diminishes, giving rise to the observed order of the flow curves.

It is rather interesting that data presented here give a clear description of the behaviour of the solutions at high shear rates, which can be complementary to the NMRI technique results obtained by Mair and Callaghan et al. [12].

Analysis of the flow curves for the different concentrations leads to conclude that there is a critical shear stress value for the onset of unstable banded flow. This shear stress value appears to be dependent on the surfactant concentration, being larger for higher concentration. Note however, that the cone and plate curves for 1.5% and 2.0% solutions show a well-defined plateau and that the time of flow in this

geometry was normally longer than the residence time in the capillaries. This suggests that a critical shear stress is not the only factor to determine the onset of banded flow since as a critical fluid residence time may be important to allow for the nucleating and growth of a second phase to lead to phase separation. The role of the fluid residence time as a critical parameter for banded flow will be explored in the following section through the dependence of flow curves on  $L/D$  capillary ratio and step shear rate experiments in cone and plate. On the other hand, clear evidence of the absence of slip has been shown, which allows to distinguish slip from constitutive instabilities. In fact, flow curves dependence on capillary diameter show the opposite phenomenon to slip, i.e., adherence. The existence of this phenomenon has not been previously reported for micellar solutions, however, it will not be discussed in detail in the present work.

### 3.2. $L/D$ dependence

#### 3.2.1. 1.5% solution

Fig. 4(a and b) describe the variation of shear stress and residence time respectively, with shear rate for capillaries of  $D = 0.12$  cm and  $L/D = 50, 100$  and  $400$  in the 1.5% solution. The flow curve of the capillary with  $L/D = 50$  lies above those of 100 and 400, which shows the influence of end effects for capillary data belonging to  $L/D = 50$ . The flow field for the capillary with  $L/D = 50$  was steady and no instabilities were observed.

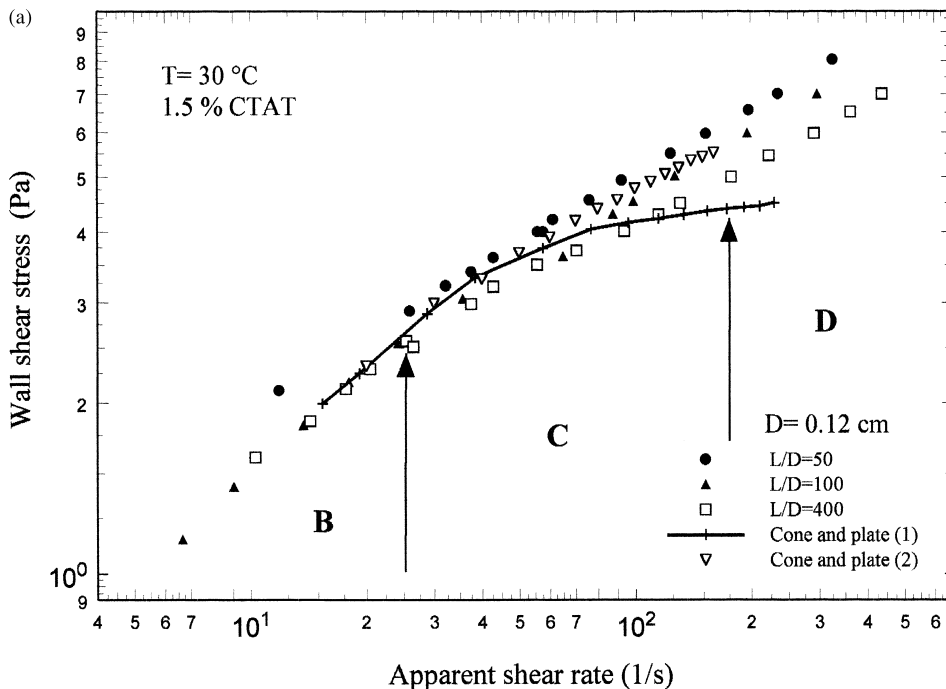


Fig. 4. (a) Apparent flow curves for the 1.5% CTAT solution obtained with different length to diameter ratios and  $D = 0.12$  cm at  $30^\circ\text{C}$ . Cone and plate (1) and (2) correspond to data obtained at 60 and 5 s after de inception of the step in the shear rate, respectively; (b) residence time as a function of the apparent shear rate for data of (a).

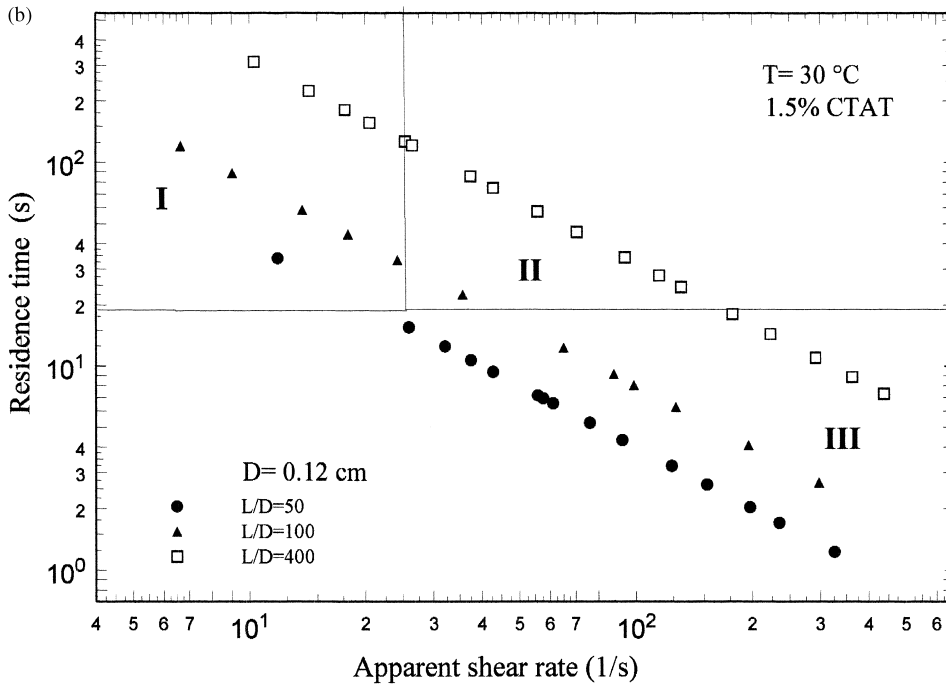


Fig. 4. (Continued)

The flow curves for  $L/D = 100$  and 400 superpose in region B which, as mentioned previously, is bounded by a shear stress of the order of 3 Pa. This fact implies that end effects are negligible for both capillaries. However, above this shear stress, in region C, data of capillaries with  $L/D = 100$  and 400 split in two flow curves that extend toward region D. In these regions, data belonging to the capillaries with  $L/D = 400$  lie below those of  $L/D = 100$ , reflecting the influence of the fluid residence time on the flow field. Once more, both regions belong to unstable flow as described before. In this section of the work, region boundaries were established with respect to the capillary of  $L/D = 400$ , the other capillaries do not have necessarily the same boundary regions because of the differences in the residence time.

In Fig. 4(b) the residence time is plotted versus the apparent shear rate. The residence time was calculated as

$$t = \frac{8L}{D\dot{\gamma}_{\text{app}}}. \quad (3)$$

The plot was divided into three regions, labelled as I, II and III, whose limits were determined by a vertical line corresponding to the shear rate at the onset of the unstable region C and by a horizontal one obtained from the shear rate at which the  $L/D = 400$  capillary leaves the unstable region C, approximately 17 s (critical time). Region I includes data obtained at low shear rates, low shear stresses and long residence times without instabilities. Region II includes data at intermediate shear rates and stresses and residence times longer than 17 s, and the most unstable flow behaviour was observed in

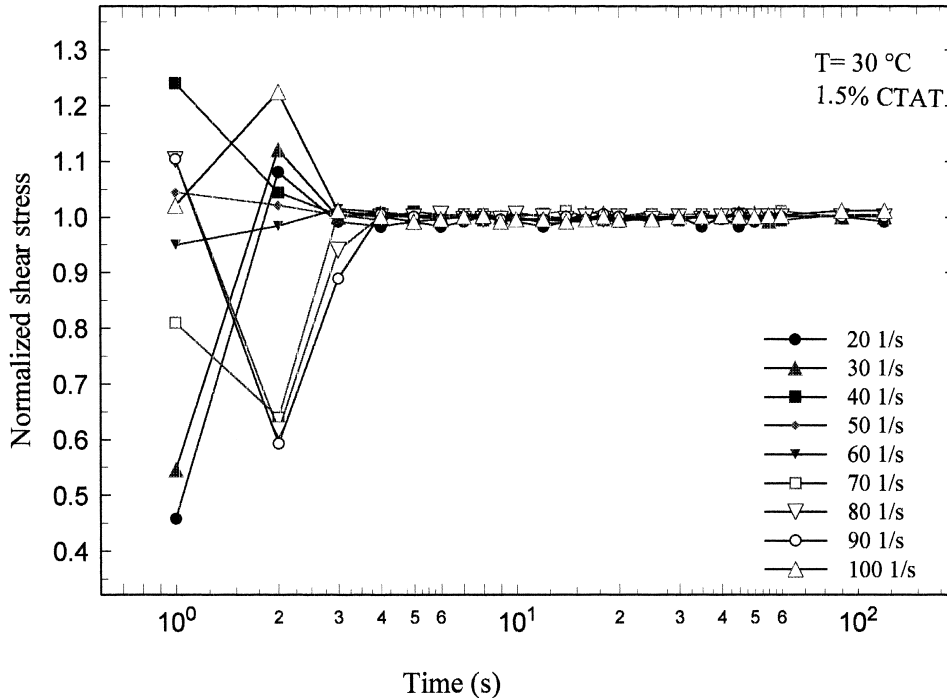


Fig. 5. Normalized shear stress as a function of time for the 1.5% CTAT solution at 30°C. Cone and plate data obtained at different shear rates.

this region. Finally, region III considers data obtained at high shear rates and stresses corresponding to low residence times. Unstable behaviour was also observed in this region only for capillaries of  $L/D = 100$  and  $400$ . This plot clearly shows that a critical shear stress and a residence time are necessary to observe unstable flow. Therefore only large enough capillaries and shear stresses trigger the unstable flow. Such a large enough residence time, of the order of 17 s, allows the nucleating and growth of a second phase on the initially homogeneous fluid, which leads to the unstable banded flow. Note that residence times in the capillary of  $L/D = 50$  are smaller than the critical value of 17 s, so the nucleation of a second phase is not permitted and instabilities are not observed.

In order to test conclusively the previous hypothesis, the study with the cone and plate rheometer was very enlightening. Experiments on the inception of flow after a step change in shear rate were carried out in the cone and plate viscometer, and the results are presented in Fig. 5. These experiments were aimed to elucidate the time scale for the attainment of steady state flow after an imposed shear rate. The utilized instrument was not sensitive enough to detect the fast transients occurring at times less than a second, but provided the required information for long times. Fig. 5 depicts the normalized stress (with respect to the value in steady conditions) versus time at the inception of the shear flow for the 1.5% solution. A careful observation of the curves for different shear rates illustrates that the steady state was not achieved before 15 s (small oscillations in the shear stress are observed at longer times, however, they are small enough to consider that the steady state has been achieved). This time scale coincides with that depicted by the horizontal line in Fig. 4(b), i.e., the line which signals the transition between the short and long residence times. It is important to note that the torque inertia did not influence the

experiments since for a Newtonian fluid (Brookfield 100) of comparable viscosity the steady state for different shear rates was reached no longer than 5 s.

Two flow curves with the cone and plate rheometer were generated taking the stress corresponding to times of 5 and 60 s after the inception of the step in the shear rate. These flow curves are plotted in Fig. 4(a) together with the flow curves belonging to different  $L/D$ . Note that the cone and plate flow curve built with data obtained 5 s after the flow inception lies close to that belonging to  $L/D = 100$  and does not show a plateau. In fact, this cone and plate flow curve looks similar in shape to that belonging to  $L/D = 50$  where small residence times are typical. However, the corresponding cone and plate flow curve built from data taken 60 s after the flow inception lies below that of  $L/D = 400$  and shows a well defined plateau. This result once more reflects the influence of the residence time and the shear stress level on the development of fluid structuration and banded flow.

3.2.2. 2% solution

Fig. 6(a and b) describe the variation of shear stress and residence time respectively, with shear rate for capillaries of  $D = 0.30$  cm and  $L/D = 50, 100$  and  $400$  in the 2.0% solution. In a similar way to the case of the 1.5% solution, the capillary flow curve for  $L/D = 50$  lies above those of  $L/D = 100$  and  $400$  in all the shear rate range studied. Also, data from  $L/D = 100$  superpose on those of  $L/D = 400$  in region B but separate in regions C and D. However, in contrast with the 1.5% solution, data from  $L/D = 50$  did show unstable flow in regions C and D. This fact can be easily observed in the Fig. 6(b),

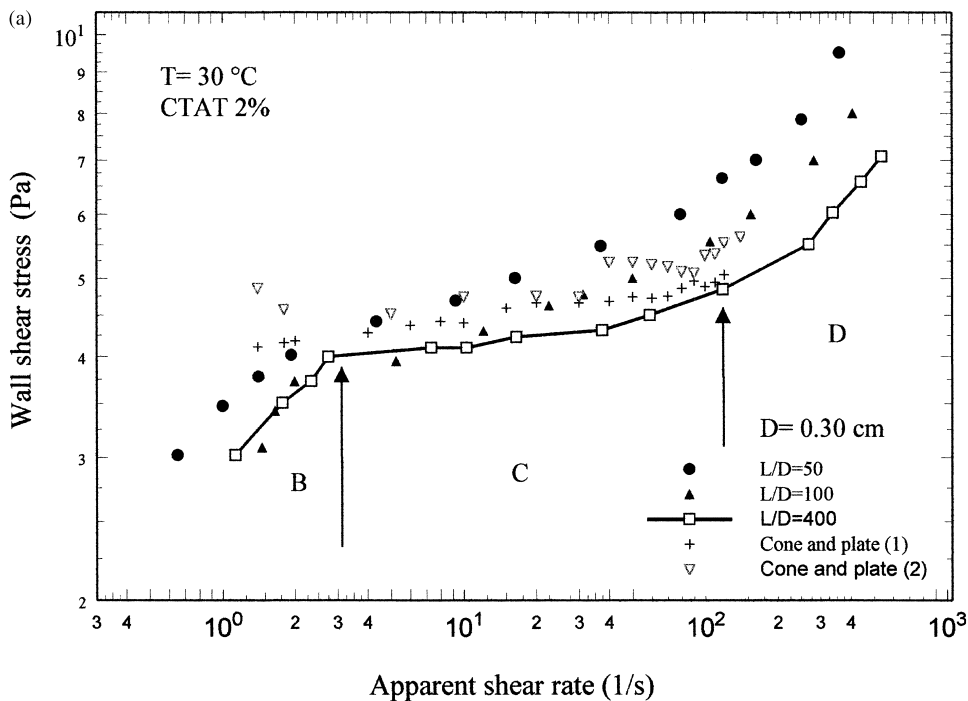


Fig. 6. (a) Apparent flow curves for 2.0% CTAT solution obtained with different length to diameter ratios and  $D = 0.30$  cm at  $30^{\circ}\text{C}$ . Cone and plate (1) and (2) correspond to data obtained at 60 and 10 s after de inception of the step in the shear rate, respectively; (b) Residence time as function of the apparent shear rate for data of (a).

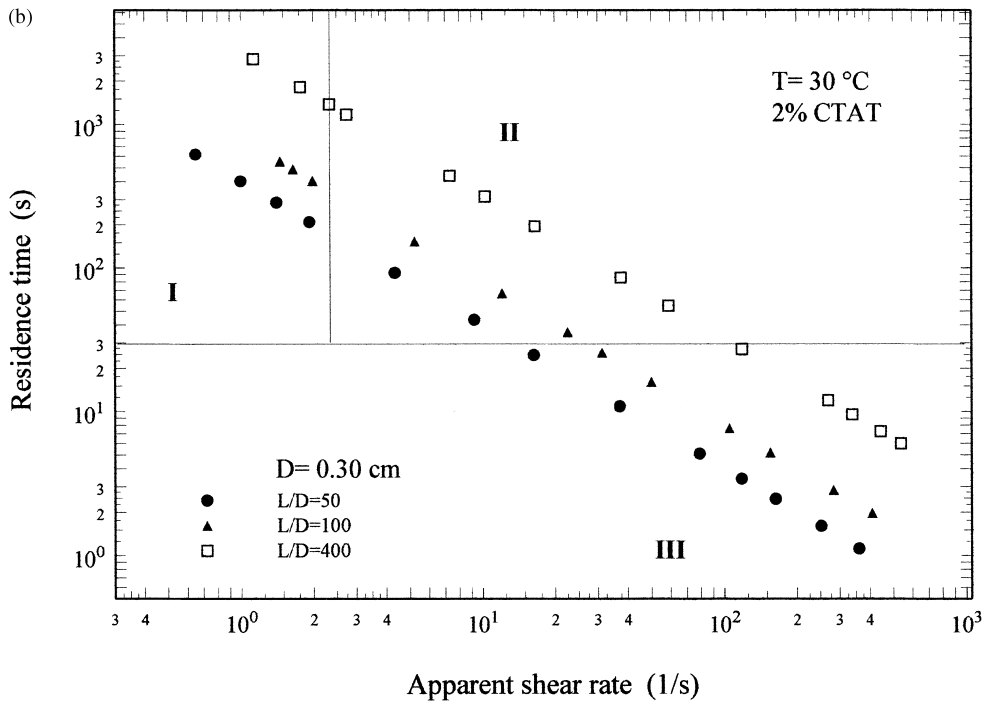


Fig. 6. (Continued)

where unstable region II and III show data belonging to  $L/D = 50$ . In this case, the horizontal line correspond to a value of around 28 s.

Cone and plate data obtained in similar conditions as described for the case of the 1.5% solution are shown in Fig. 7(a and b). The steady state was achieved in this case at flow times of the order of 30 s, which is very similar to the time defining the horizontal line in Fig. 6(b). Cone and plate data obtained 10 s after the flow inception lie above those taken at 60 s. Note that cone and plate data taken after 10 s are not steady values, however, those obtained 60 s after the inception did show the plateau.

The regions of instability and those where banded flow develops in the capillary flow of these solutions is therefore dependent on both the magnitude of the stress and the residence time of the solution in the flow system. Banded flow occurrence is thus, a time dependent phenomenon. According to Berret [15,16], during fast transient or for very short times, the fluid is homogeneous. As time proceeds, after a critical period there is a possibility that banded flow develops and the fluid becomes non-homogeneous [12]. As observed in Fig. 6(b) and Fig. 7(a and b), the time scale for the attainment of steady state flow is located at the transition from short to long residence times, approximately 27 s, which actually coincides with the high shear rate limit of the plateau.

From the previous results, it can be clearly concluded that not only a critical shear stress is needed to trigger the banded flow, but also a critical residence time is necessary to allow for the nucleation and growth of a second phase that leads to flow instabilities.

Finally, it is worth noting that in spite of the large  $L/D$  used in this work, the maximum viscous heating calculated assuming adiabatic conditions is of the order of  $0.001^\circ\text{C}$ . Therefore, the experiments

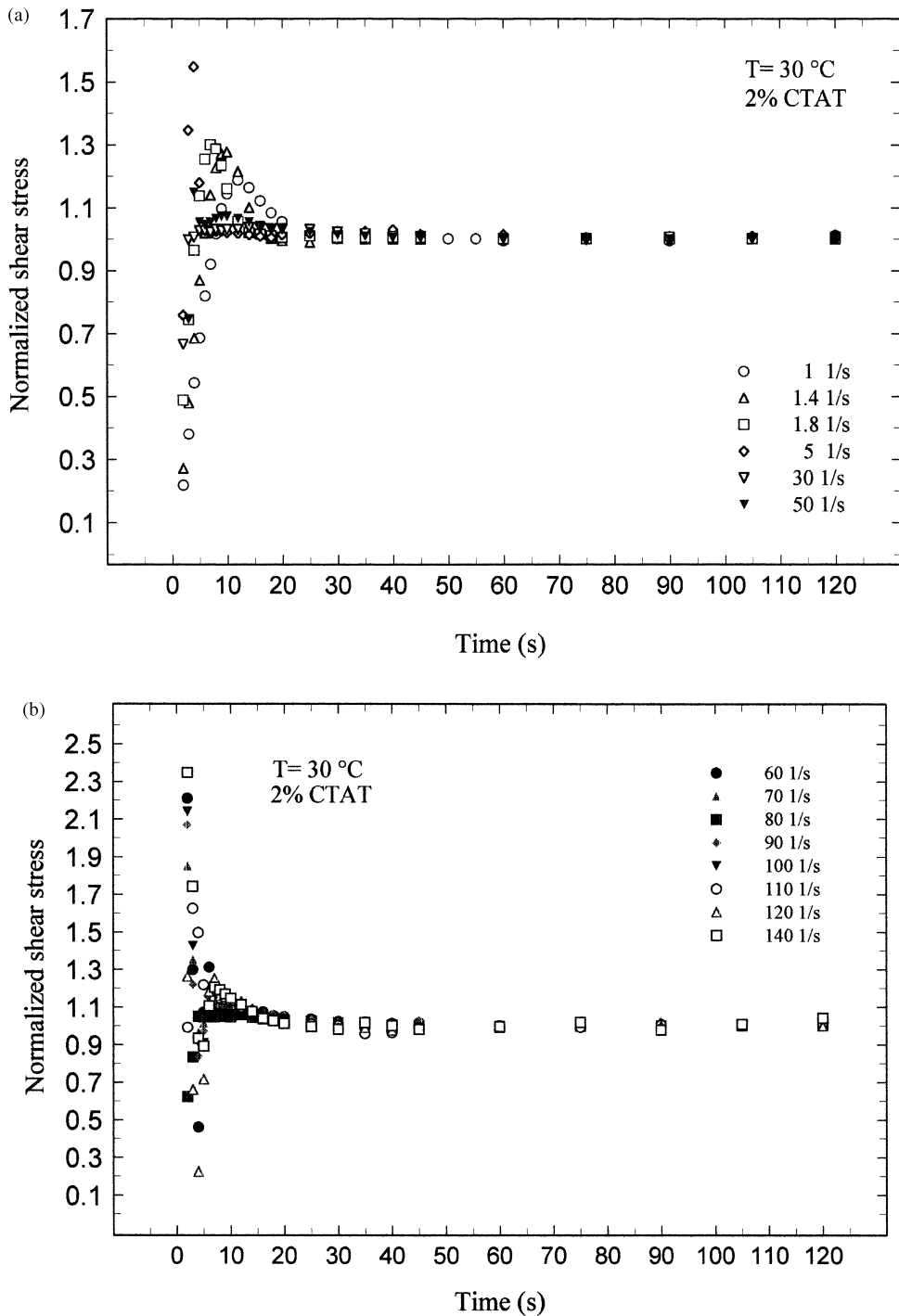


Fig. 7. Normalized shear stress as a function of time for the 2.0% CTAT solution at 30°C. Cone and plate data obtained for different shear rates. (a) low shear rates; (b) high shear rates.

were performed under isothermal conditions and viscous heating does not have any effect on the results.

### 3.3. Flow visualization

As observed in the previous data, an important cause of the flow instabilities which lead to the presence of ‘banded flow’, is the time allowed for the fluid structuration. A series of visualization

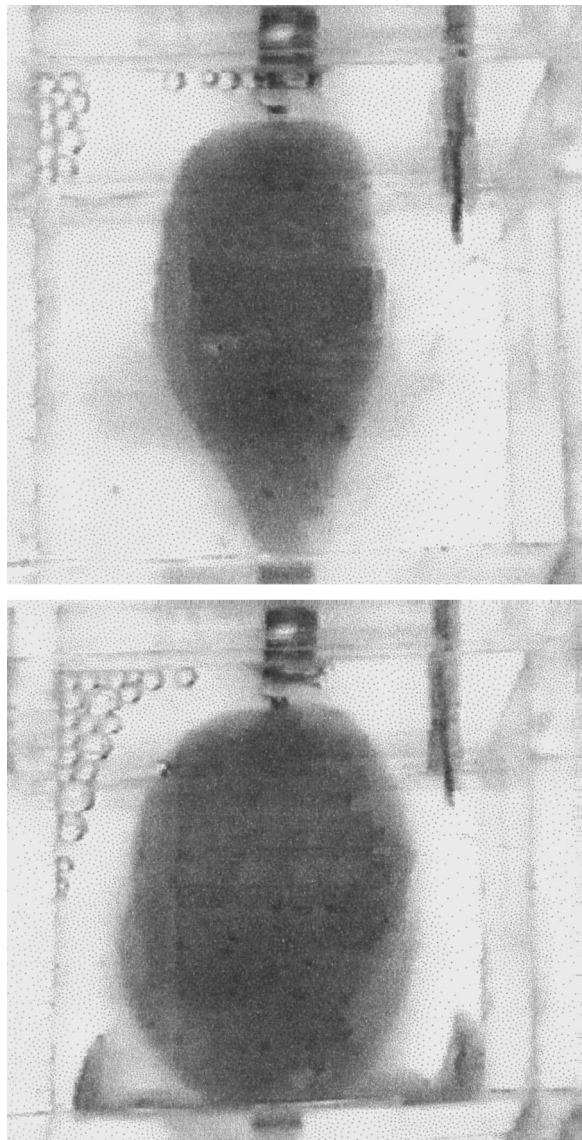


Fig. 8. Flow patterns close to the capillary entry for the 2.0% solution at different times. Note the development of vortices typical of elastic liquids.

studies were carried out by permitting a large residence time of the fluid in the flow system. Such a large residence time was obtained by using a long hose placed between the pressure box and the reservoir where the capillary was connected, as described in the experimental section. The setup allowed residence times of the order of an hour, which are sufficient for the development of banded flow. For observations of the flow pattern in the reservoir where the capillary is connected, a dye was mixed with the solution. The different stages of the flow development were recorded by a video-camera placed at different observation angles.

For the 1.5% CTAT solution, the Fig. 8(a and b) shows photographs of the evolution of a flow pattern clearly expanded into a globular region. There is a profound change in the expansion and contraction regions, especially in the latter, where large vortices characteristic of elastic liquids form close to the capillary entrance. Although it is not distinguished in the figure, it was observed during the experiments that the fluid developed another structure in the vortex region, which was identified by differences in the refraction index with respect to the rest of the solution.

Another important effect found in the 2% solution concerns with the existence of a small window of critical stresses located just above the transition from power-law behaviour into the plateau region, at approximately 3 Pa, where the time for attainment of steady state appeared extremely long. With the long hose, it was observed that the flow rate began to increase with a continuously decreasing pressure as measured in the transducer located at the capillary entrance, even though the driving pressure provided in the first box was kept constant. As observed in Fig. 9, where the shear stress versus shear

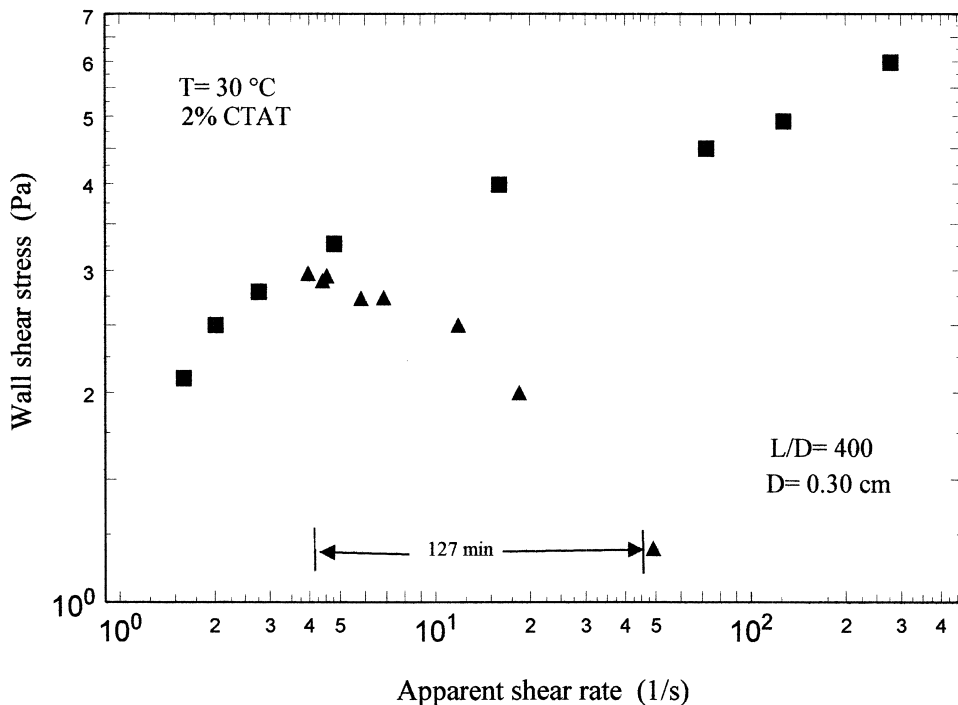


Fig. 9. Flow curve for the capillary with  $L/D = 400$  and  $D = 0.30$  cm. Triangles belong to data taken at different times at the onset of the unstable flow region. Note that unstable data began at the flow curve and then moved downward until a minimum was reached. Such a minimum was coincident with a striking spurt flow. Time elapsed during the gathering of these data is of the order of 127 min.

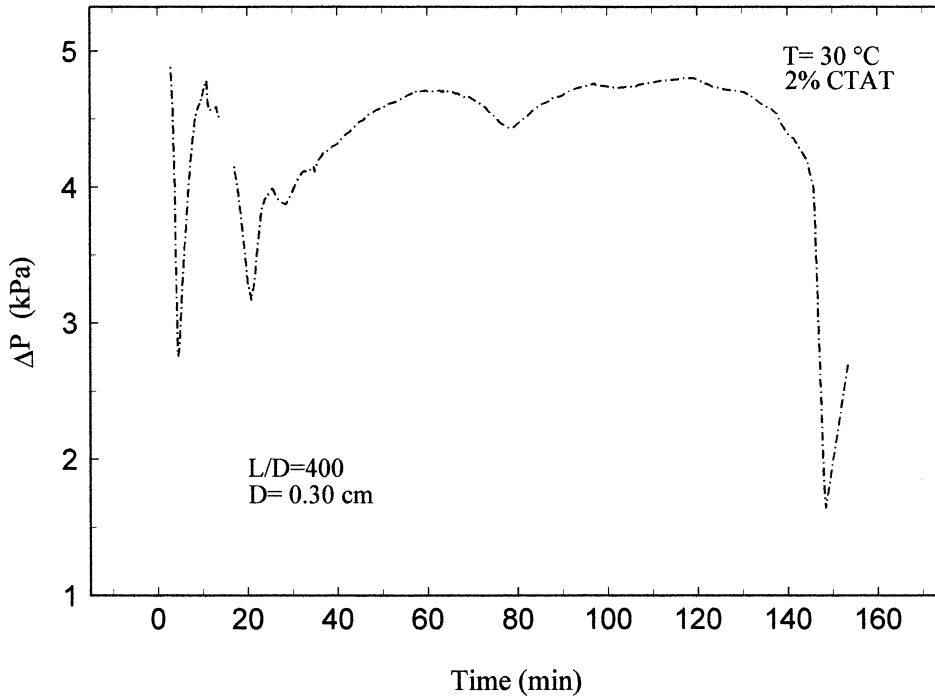


Fig. 10. Pressure drop variations during the time of gathering the unstable data of Fig. 9.

rate data for the capillary with 0.30 cm diameter are shown, a decreasing unstable branch initiates at the above stress corresponding to a shear rate of about  $3.5 \text{ s}^{-1}$  and ends at almost 1 Pa ( $50 \text{ s}^{-1}$ ). These data were gathered during the time interval of pressure variations. The corresponding variation of the stress as a function of time is illustrated in Fig. 10, while the flow rate instability is presented in a series of photographs in Fig. 11(a and d). In a time scale of the order of an hour, the pressure oscillated from about 5 kPa down to approximately 3 kPa. After two oscillations, the pressure nearly recovers its initial value and remains at this level for almost 90 min. From now on, the pressure decreases first slowly and past a critical value, a dramatic drop lasting about 4 min was observed. After reaching the pressure of 1.7 kPa, a rebound is seen and the pressure increased again to stress values around to 3 Pa. The corresponding variation in the flow rate is observed in figures (Fig. 11(a–d)). As the pressure decreases from 4.86 to 2.77 kPa, the liquid drops emerge from the capillary change into a continuous discharge. As soon as the pressure starts to increase once more, the flow rate decreases and the liquid emerging from the capillary changes into a drop-like motion. The whole process lasted more than an hour, and subsequently, instead of becoming stable flow, it began to decrease once more. There was not evidences of the attainment of an steady state from the data gathered. The stress window was difficult to locate and only could be resolved in the 2% solution.

From the results presented above, it is reasonable to suggest that the instabilities observed in this solution after a long residence time in the flow system are representative of a banded flow, since the shear rate oscillates between a low value ( $3.5 \text{ s}^{-1}$ ) and a high value ( $50 \text{ s}^{-1}$ ) as soon as a critical stress is reached. The period of the oscillations is very long, over a time scale of the residence time of the liquid in the flow system. Along the decreasing part of the cycle, the flow rate showed an extraordinary

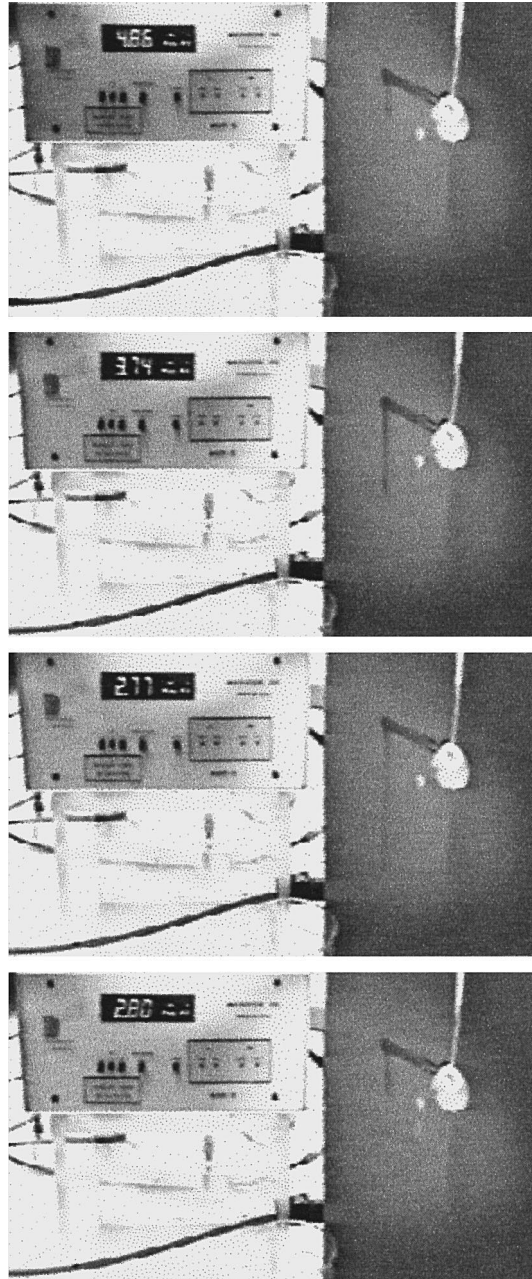


Fig. 11. Images at different times of the spurt instabilities. Note the increase in the flow rate along with the decrease in the pressure drop and viceversa.

jump, which occurs during the last part of the pressure drop before reaching the minimum in the pressure. This increase occurs after the liquid has flown from the beginning of the first box up to the capillary entrance, suggesting an induction period for band formation before a sudden increment in

flow rate. Since the residence time in the flow system is 66 min and the dramatic pressure drop, which accompanies the sudden increase in flow rate, occurs during the last 4 min, the induction time is 62 min for this solution. It is remarked that this effect is observed at constant driving pressure.

#### 4. Conclusions

The capillary flow of wormlike micellar systems presents a unique rheological behaviour which is dependent on the residence time of the liquid in the capillary and on a critical shear stress. Long residence times may induce a plateau-like region in the flow curves, as well as flow instabilities which have been attributed to the existence of banded flow and are accompanied by dramatic spurt flow. This experimental study has shown the close interrelation existing among shear stresses and residence times for the appearance of instabilities and the onset of structuration in the fluid.

It has been shown that non-monotonic flow curves for these micellar systems, consistent with constitutive instabilities, may be observed in the absence of slip. In fact, for the CTAB solutions used through this work, the opposite phenomenon appears to occur, i.e., adherence.

The results derived from this work can contribute to the understanding of the development of banded flow from an initially homogeneous fluid, as well as to distinguish between constitutive instabilities and slip.

#### Acknowledgements

We acknowledge to DEPI-IPN for the financial support to perform this work. L de V. and J. P-G are COFAA Fellows. S. H-A received a CONACyT scholarship to perform this work. We want to acknowledge the referees for useful comments.

#### References

- [1] H. Rehage, H. Hoffmann, Rheological properties of viscoelastic surfactant systems, *J. Phys. Chem.* 92 (1988) 4712.
- [2] H. Rehage, H. Hoffmann, Viscoelastic surfactant solutions: model systems for rheological research, *Mol. Phys.* 74 (1991) 933.
- [3] N.A. Spenley, M.E. Cates, T.C.B. MacLeish, Nonlinear rheology of wormlike micelles, *Phys. Rev. Lett.* 71 (1993) 939.
- [4] J.F. Berret, D.C. Roux, G. Porte, Isotropic-to-nematic transition in wormlike micelles under shear, *J. Phys. II (France)* 4 (1994) 1261.
- [5] R. Makhloufi, J.P. Decruppe, A. Ait-Ali, R. Cressely, Rheo-optical study of wormlike micelles undergoing a shear banding flow, *Europhys. Lett.* 32 (1995) 253.
- [6] J.P. Decruppe, R. Cressely, R. Makhloufi, E. Cappelare, Flow birefringence experiments showing a shear-banding structure in a CTAB solution, *Colloid Polym. Sci.* 273 (1995) 346.
- [7] V. Schmitt, F. Lequeux, A. Pousse, D. Roux, Flow behaviour and shear-induced transition near anisotropic–nematic transition in equilibrium polymers, *Langmuir* 10 (1994) 955.
- [8] J.F. Berret, D.C. Roux, G. Porte, P. Lindner, Shear-induced isotropic-to-nematic phase transition in equilibrium polymers, *Europhys. Lett.* 25 (1994) 521.
- [9] E. Cappelare, R. Cressely, J.P. Decruppe, Linear and non-linear rheological behaviour of salt free aqueous CTAB solutions, *Colloids Surf.* 104 (1995) 353.

- [10] P.T. Callaghan, M.E. Cates, C.J. Rofe, J.B.F. Smeulders, A study of the spurt effect in wormlike micelles using nuclear magnetic resonance microscopy, *J. Phys. II (France)* 6 (1996) 375.
- [11] D. Ohlendorf, W. Interthal, H. Hoffmann, Surfactant systems for drag reduction: physico-chemical properties and rheological behaviour, *Rheol. Acta* 25 (1986) 468–486.
- [12] R.W. Mair, P.T. Callaghan, Shear flow of wormlike micelles in pipe and cylindrical couette geometries as studied by nuclear magnetic resonance microscopy, *J. Rheol.* 41 (1997) 901.
- [13] J. Pérez-González, L.de Vargas, J. Tejero, Flow development of xanthan solutions in capillary rheometers, *Rheol. Acta* 31 (1992) 83.
- [14] W. Kozicki, S.N. Pasari, A.R.K. Rao, C. Tiu, Anomalous effects in laminar capillary flow of polymer solutions, *Chem. Eng. Sci.* 25 (1970) 41–51.
- [15] J.E. Berret, Transient rheology of wormlike micelles, *Langmuir* 13 (1997) 222.
- [16] J.F. Berret, D.C. Roux, Rheology of nematic wormlike micelles, *J. Rheol.* 39 (1995) 725–741.